KURENAI
Kyoto University Research Information Repository

KYOTO UNIVERSITY

Title	Second-harmonic resonance with parametric excitation : degenerate "bouncing" solutions (Mathematical Aspects on Waves of Strong Nonlinearity or Large Degrees of Freedom)
Author(s)	Craik, A.D.D.
Citation	(1999), 1092: 11-21
Issue Date	1999-04
URL	http://hdl.handle.net/2433/62937
Right	
Type	Departmental Bulletin Paper
Textversion	publisher

Kyoto University

Second-harmonic resonance with parametric excitation: degenerate "bouncing" solutions.

A.D.D. Craik

School of Mathematical & Computational Sciences,

University of St Andrews, St Andrews, Fife KY16 9SS,

Scotland, U.K.

and

Research Institute for Mathematical Scieences,

Kyoto University, Kyoto 606-01, Japan.

Abstract

The equations

$$da/dt = -\sigma a + \mu a^* + \lambda a^* b, \qquad db/dt = -\sigma_1 b + \nu a^2$$

describe perfectly-tuned second-harmonic resonance of two small-amplitude standing water waves with Faraday excitation. Identical equations are also found for forced, resonant, coupled pendula. Though more general equations, that incorporate frequency detuning, have previously been examined, analytical progress is then hard.

By assuming perfect tuning, and very weak damping ($\sigma_1 \ll 1$) of the b-wave, a virtually complete description of the solution trajectories is found. The degenerate case $\sigma_1 = 0$ has a *continuum* of fixed points, and the solutions then take an unusual form: several "bounces" are separated by pauses at unstable fixed points, until small random disturbances grow and initiate the next "bounce". This continues until a "bounce" terminates at a stable fixed point. When σ_1 is small but non-zero, a similar qualitative structure remains; but all solutions eventually terminate at one of a pair of stable fixed points of the now non-degenerate system.

When σ_1 is imaginary, the equations describe detuning from internal resonance: when this is small, similar arguments apply.

----

1. Introduction

The equations here investigated arise for an idealisation of Faraday water waves, and also for forced, coupled simple pendula, at precise second-harmonic resonance (see Miles 1984, 1985, Gu & Sethna 1987, Henderson & Miles 1991, Forster & Craik 1997). With only the two resonant modes present, their rapid periodic oscillations may be factored out, leaving a pair of coupled evolution equations, on a much longer timescale t; namely,

$$da/dt = -\sigma a + \mu a^* + \lambda a^* b, \qquad db/dt = -\sigma_1 b + \nu a^2. \qquad (1)$$

Here, a, b are suitably-scaled complex amplitudes of the two participating modes with natural frequencies in the ratio 1:2 on the eliminated short timescale. Mode a is linearly damped, with damping rate σ, and it is parametrically forced by a small externally-imposed periodic oscillation with frequency exactly twice that of mode a. The amplitude of this forcing is represented by the real parameter μ. Wave b is not directly forced, and it has a linear damping rate σ_1 which, in this paper, is mostly assumed to be small compared with σ. The nonlinear resonance interaction coefficients λ, ν may be taken as real without loss, and have opposite signs. The * denotes complex conjugate. When the waves are slightly detuned from internal resonance, the coefficient σ_1 has an additional imaginary part $-i\varepsilon$, say, which is proportional to $\omega_2 - 2\omega_1$, where ω_1 and ω_2 are the natural frequencies of the two modes on the fast timescale. Details of the derivation of these equations can be found in the works cited above.

In fact, these previous works mostly consider a more general pair of equations, that admits further slight detuning of the wave frequencies from the driving frequency. That is to say, the parametric (Faraday) forcing frequency, and the frequency of mode b, are both allowed to differ slightly, and independently, from twice that of mode a. The bifurcation structure of fixed points of this more general pair of equations has been studied in detail; and some properties of the solution trajectories may be inferred from this structure. In particular, Gu & Sethna (1987) have proved the existence of chaotic orbits, when both types of detuning are present. However, in such cases, a complete theoretical description of the solution trajectories is unavailable.

The present paper addresses only the simpler set of equations (1), for which real progress can be made. For the degenerate case $\sigma_1 = 0$ described in section 2, we are able to infer the complete solution structure, which is intermittently affected by the presence of small disturbancs. Then, in sections 3 and 4, we examine cases with real and imaginary non-zero σ_1, finding qualitative similarities with the degenerate case.

2. Degenerate cases $\sigma_1 = 0$

Provided μ is non-zero, equations (1) with $\sigma_1 = 0$ may be rescaled to

$$da/dt = -\sigma a + a^* - a^* b, \qquad db/dt = a^2. \qquad (2)$$

Stationary points are $(a, b) = (0, k)$ where k is an *arbitrary* complex constant. The degeneracy therefore introduces a continuum of fixed points, absent when σ_1 is non-zero. Each of these points is found to be linearly stable when k lies in the complex b-plane within a circle of radius σ and centre $(1, 0)$.

The case $\sigma = 0$ reduces, on writing $c = b - 1$, to the equivalent *unforced* equations,

$$da/dt = -a^* c, \qquad dc/dt = a^2,$$

which have $a^2 + c^2$ = constant. Full solutions are then known in terms of elliptic functions. Therefore, *the forced undamped system is dynamically equivalent to the unforced undamped system*, with only a translation of variables ($c = b + \mu/\lambda$ in the original system): this was already noted by Forster & Craik (1997).

For $\sigma > 0$, we instead have

$$da/dt = -\sigma a - a^*c, \qquad dc/dt = a^2, \qquad (3)$$

and $d(aa^* + cc^*)/dt = -2\sigma aa^* \leq 0$. Therefore, the "distance" from $(a, b) = (0, 1)$ in the 4-dimensional double complex planes of a, b is non-increasing; and it is strictly decreasing whenever a is non-zero. It follows that all trajectories must eventually terminate at a stable fixed point with $a = 0$, somewhere within the circular domain of the b-plane just described.

Also, since the equations (3) are invariant under the phase-shifts $(a, c) <\text{->} (ae^{i\delta}, ce^{2i\delta})$, we may choose (say) ph(a) to be initially zero, without loss of generality; and recover many other cases from the mapping. However, these apparently innocuous phase shifts require care. For instance, an initial state $a = \varepsilon$ (small, real and positive) and $b = 0$ ($c = -1$) experiences initial amplification of a, as $\varepsilon\exp(1-\sigma)t$ whenever $\sigma < 1$; but phase shift of a alone by $\delta = \pi/2$ yields initial *decay* as $i\varepsilon\exp(-1-\sigma)t$ when $b = 0$. In fact, the transformation $c <\text{->} ce^{2i\delta}$ requires the new b to be 2, not 0, for which the appropriate growth of a results.

First, we restrict attention to cases where b is initially zero, and a grows from infinitesimal levels. Clearly, the linearly most unstable a-disturbance is then likely to dominate. Such linear growth occurs whenever $\sigma < 1$, and the most-amplified disturbances have wholly-real a. Both a and b remain real for later times t, at least until another stationary point is reached. From (2), the corresponding pair of *real* equations is then

$$da/dt = a(1 - \sigma - b), \qquad db/dt = a^2.$$

These have (2-dimensional) fixed points $(a, b) = (0, K)$ for arbitrary real K; and trajectories lie on the semicircles $a^2 + (b+\sigma-1)^2$ = constant ($a \geq 0$ or $a \leq 0$), all of which terminate on fixed points with $a = 0$. The trajectory that corresponds to our assumed initially-small a and b terminates at $b = K = 2(1 - \sigma)$.

However, we have shown above that such fixed points in the *four-dimensional* plane are stable only when $1 - \sigma < K < 1 + \sigma$. The value $K = 2(1 - \sigma)$ lies outside this range whenever $\sigma < 1/3$. So what happens when this (or any other) trajectory terminates at an unstable fixed point? The answer is that another infinitesimal instability must develop; and, since $K > 1 + \sigma$, the dominant growing disturbance now has a purely imaginary. Writing $a = ia'$, we obtain another pair of *real* equations,

$$da'/dt = a'(-1 - \sigma + b), \qquad db/dt = -a'^2.$$

These have the same fixed points as before; but trajectories given by the different semicircles $a'^2 + (b-\sigma-1)^2 = \text{const.}$ ($a' \geq 0$ or $a' \leq 0$).

Our initially-infinitesimal solution therefore proceeds from $(a, b) = (0, 0)$ to $(0, 2(1-\sigma))$ along the upper or lower semicircle. If $\sigma < 1/3$, it then must wait for infinitesimal disturbances to grow and force it onto another trajectory in the orthogonal (a', b) plane: this is one of the two semicircles $a'^2 + (b-\sigma-1)^2 = (1-3\sigma)^2$, ($a' \geq 0$ or ≤ 0), which terminates at $b = 4\sigma$, $a = 0$. This is a stable fixed point provided $1/5 \leq \sigma \leq 1/3$. But, if $\sigma < 1/5$, there will be a further wait for amplification of real a-disturbances, before the trajectory proceeds along the corresponding semicircle, $a^2 + (b+\sigma-1)^2 = (5\sigma - 1)^2$, to the fixed point $(0, 2(1 - 3\sigma))$. This is stable if $1/7 \leq \sigma \leq 1/5$, but unstable if $\sigma < 1/7$. It is readily shown that the composite trajectory, starting at $(0, 0)$ and subject to arbitrary infinitesimal disturbances, consists of N ($= 1,2,3, ...$) "bounces" when $1/(2N + 1) \leq \sigma \leq 1/(2N - 1)$; or, equivalently, $\sigma^{-1} - 1 \leq 2N \leq \sigma^{-1} + 1$. The corresponding end-points of the trajectories have $b_{2M} = 4M\sigma$, $b_{2M+1} = 2 - 2(2M + 1)\sigma$, where $M = 0, 1, 2,...$ until $2M$ or $2M+1$ equals N.

More generally, real initial data $(a, b) = (0, K)$, for any $K = b_0$ *less* than $1 - \sigma$, give subsequent endpoints $b_{2M} = K + 4M\sigma$, $b_{2M+1} = 2 - K - 2(2M + 1)\sigma$; and initial data $(a, b) = (0, K)$, for any $K = b_0$ *greater* than $1 + \sigma$, give subsequent endpoints $b_{2M} = K - 4M\sigma$, $b_{2M+1} = 2 - K + 2(2M + 1)\sigma$. These sequences terminate as soon as a b_n falls within the stable interval $[1 - \sigma, 1 + \sigma]$. A composite picture is shown in Figure 1 for the "four-bounce" case $\sigma = 1/8$ with zero initial data: the arrows indicate direction of motion as time increases. The clockwise semicircular trajectories are in the real (a, b) plane, and the anti-clockwise ones in the orthogonal (a', b) plane: the b-axis is horizontal, and the a or a' axis is vertical. Though all semicircles are drawn in the upper half plane, any might instead be in the lower half-plane, if the appropriate linearly-growing small disturbance of a or a' were negative rather than positive.

Corresponding trajectories for *any* initial data having a either wholly real or wholly imaginary, and b wholly real, may be inferred similarly, since the initial data identifies the appropriate circle for the trajectory's first "bounce". Additional families of trajectories may be deduced from the invariant mapping $(a, c) \leftrightarrow (ae^{i\delta}, ce^{2i\delta})$. In fact, this tells us much about *all possible trajectories*. For, it was shown for equations (3) above that, whenever $\sigma > 0$, arbitrary initial complex values of (a, c) must eventually reach a fixed point with $a = 0$ and c equal to some complex constant $k = Ke^{i\delta}$. The trajectory that arrives at this point may well *not* have had a and c in a fixed phase relationship $2ph(a) = ph(c)$ or $ph(c) + \pi$ [mod(2π)]: therefore, we are unable to determine this initial portion of the evolution except by direct computation. But, after every such trajectory has reached a fixed point with $a = 0$, we can now determine the nature of the subsequent behaviour. The *next* "bounce" (if there is one) will be determined by the fastest-

growing linear disturbance, and this corresponds to a trajectory like those just found, if we first apply the mapping to make c real. For example, a trajectory that has reached $a = 0$, $c = 1 + 3^{1/2}i$ may then be transformed to the dynamically-equivalent $a = 0$, $c = 2$ by the phase mapping. The subsequent (but *not* the earlier) evolution is therefore dynamically equivalent to that emanating from $a = 0$, $b = 3$; and this has been deduced above.

Of course, since the instability of fixed points depends on unknown small disturbances, the "waiting time" spent in the vicinity of such points is not known without specifying the level of such disturbances; nor is it known which of the two available semicircular trajectories will be followed, unless the sign of the a-disturbance is also specified. But it is surprising that so much can be deduced so simply.

3. Cases with non-zero σ_1

When σ_1 is non-zero, the corresponding scaled equations are

$$da/dt = -\sigma a + a^* - a^*b, \qquad db/dt = -\sigma_1 b + a^2. \qquad (4)$$

Now the degeneracy is removed, and the continuum of fixed points disappears. Instead, provided $0 < \sigma < 1$ and $0 < \sigma_1$, the only fixed points remaining are $(a, b) = (0, 0)$, and the pair

$$a = \pm[(1 - \sigma)\sigma_1]^{1/2} \qquad b = 1 - \sigma. \qquad (5)$$

The origin $(0, 0)$ is unstable to parametric forcing since $0 < \sigma < 1$. As the equations (4) are invariant under the mapping $a <-> -a$, the pair of points (5) are identical in nature. It is readily shown that they are stable fixed points: their four exponents are

$$(1/2)[-\sigma_1 \pm (\sigma_1{}^2 - R)^{1/2}], \qquad (1/2)\{-2\sigma -\sigma_1 \pm [(2\sigma - \sigma_1)^2 - R]^{1/2}\},$$

where $R = 8\sigma_1(1 - \sigma)$. All four exponents are real and negative when $0 < (1 - \sigma) < \sigma_1/8$; but, when $0 < \sigma_1/8 < (1 - \sigma)$, the first pair are complex conjugates with negative real part, corresponding to damped oscillations. When σ_1 approaches zero, three of the four exponents also approach zero.

It is natural to ask how the solution structure described above, when $\sigma_1 = 0$, is modified by the presence of a *small* positive damping rate σ_1. The continuum of points $(a, b) = (0, k)$, for arbitrary k, are no longer equilibria: instead, when $a = 0$, the modulus of b decays with the exponential rate σ_1. When, previously, a "bounce" terminated at an unstable fixed point, the solution remained there until infinitesimal disturbances of a were amplified to significant levels, with a "waiting time" depending only on the available small disturbances. Now, however, a solution reaching such a point is subject to two effects: rather than simply "waiting" at a fixed b-

value, the value of b will be subject to a slow exponential decay during the growth of small unstable a-perturbations. How much the b-value is reduced before the trajectory takes off on another "bounce" is influenced by the size of small disturbances. Accordingly, without knowing the latter, it is impossible to determine the precise starting point of the next "bounce"; although we know, to good approximation, what that "bounce" must be, once its starting point is fixed. However, provided the "waiting time" for growth of small a-disturbances to significant levels is much smaller than σ_1^{-1}, we can be sure that the succession of "bounces" is not much altered from the case with $\sigma_1 = 0$, until the solution reaches a stable fixed point of the continuum. We recall that such stable fixed points have values of k, in the complex b-plane, that lie within a circle of radius σ and centre $(1, 0)$.

From then on, the only significant change in the solution is the slow exponential decay of the b-mode, with $a = 0$, until the modulus of b approaches its smallest available stable value. When b is real, this smallest value is $1 - \sigma$; but, for non-zero σ_1, there is no invariant mapping $(a, c) <-> (ae^{i\delta}, ce^{2i\delta})$ to permit reduction of all complex cases. Consequently, we are here content to illustrate the behaviour for purely real values of b.

As b comes close to its smallest stable value of $1-\sigma$, the solution enters its final approach to one or other stationary point (5). Small a-disturbances grow when b falls below $1-\sigma$. The growing a-disturbances are necessarily real, and the solution trajectory finally spirals in to the stationary point. An example of this final approach, for $\sigma = 0.5$ and $\sigma_1 = 0.01$, is shown in Figure 2. The solution at first moves along the b-axis from 1.2 (in fact, with a very small initial positive a-value), and the motion is then clockwise as time t increases, eventually approaching the fixed point $(a, b) = (1/10\sqrt{2}, 1/2)$.

Figure 3a shows a sample of computed trajectories for $\sigma = 0.2$ and $\sigma_1 = 0.01$. The horizontal axis denotes b, which is taken to be real; the positive vertical axis denotes wholly-real a (which may be either positive or negative); and the negative vertical axis denotes the magnitude of purely imaginary a (again positive or negative). In each half-plane, the appropriate real equations were solved numerically. The curves in both half-planes are traversed clockwise as t increases.The near-semicircular structure is very similar to that obtained with $\sigma_1 = 0$. But undisturbed trajectories in the upper half-plane must all eventually approach the spiral sink at $(\pm a, b) = (0.08944, 0.8)$. However, in the presence of small disturbances, it is still possible for "bouncing" to occur, with alternately real and imaginary a-values. Figure 3b shows corresponding sets of trajectories in the more heavily-damped case $\sigma = \sigma_1 = 0.2$. The spiral structure is more marked, with the sink at $(\pm a, b) = (0.4, 0.8)$. Far larger disturbances would now be needed to divert a trajectory from the upper half plane to the lower. Undisturbed trajectories in the lower half-plane all eventually approach $(a, b) = (0, 0)$: but, since this equilibrium point is unstable to real a-disturbances, the trajectory must eventually continue into the upper half-plane, and so towards a spiral sink.

The sensitivity of solutions to small disturbances, when they approach close to the b-axis, is doubtless part of the reason why chaos is sometimes found when slight frequency-detuning is added to the equations: see Gu & Sethna (1987). Although our equations (1) do not support chaos, and the structure of fixed points could hardly be simpler, trajectories when σ_1 is small can nevertheless exhibit unpredictable "waiting times" and "bounces" when random external disturbances are present.

4. Detuning from internal resonance

When the waves are not quite resonant, suitably-scaled equations corresponding to (2) are

$$da/dt = -\sigma a + a^* - a^* b, \qquad db/dt = i\varepsilon b + a^2. \qquad (6)$$

Here, the b-wave is once more considered to be undamped, and the real parameter ε measures the extent of detuning from internal resonance: see e.g. Miles (1984), Forster & Craik (1997) for details.

The only stationary points are now the origin $(a, b) = (0, 0)$, which is a saddle point when $0 < \sigma < 1$, and $(\pm a_0, b_0)$, where

$$a_0 = (\varepsilon/2)^{1/2}(1 - \sigma^2)^{1/4}[(1 + \sigma)^{1/2} - i(1 - \sigma)^{1/2}],$$
$$b_0 = (1 - \sigma^2) + i\sigma(1 - \sigma^2)^{1/2}. \qquad (7)$$

These points agree with results of Gu & Sethna (1987), who showed that the latter are stable sinks. (They found more exotic behaviour when there is detuning also of the driving frequency, but such effects are not considered here.)

There are simple periodic orbits $(a, b) = [0, K\exp(i\varepsilon t)]$ for arbitrary complex constants K. Small a-perturbations to such orbits are governed by

$$da/dt + \sigma a = a^* [1 - K\exp(i\varepsilon t)]. \qquad (8)$$

The stability of this 2-dimensional linear system with time-periodic coefficients may readily be determined by Floquet theory; but details are not given since instability is intuitively evident for all $\sigma < 1$. To illustrate this, recall that, for *fixed b*, a-disturbances are unstable whenever b lies outside the circle in the complex plane with centre 1 and radius σ. But, when $b = K\exp(i\varepsilon t)$, orbits pass through this circle only temporarily, if at all. To verify this, sample computations were performed with variables $X = \text{Re}\{\mu\}$, $Y = 2\text{Im}\{\mu\}$, where $a = C\exp[\mu(t)]$ and C is an arbitrary complex constant. Figures 4a,b,c show trajectories (X, Y) for the three cases $K = 0.5$, 1.0 and 1.5 respectively, with $\sigma = 0.5$ and $\varepsilon = 0.1$. Both growing modes (upper curves) and decaying modes (lower curves) are found, the latter being computed by reversing the time direction. Clearly, these correspond to growing and decaying Floquet modes. Though case (b) shows small 'loops' where the instantaneous growth rate X is briefly negative, strong overall

growth is evident in all cases. The phase Y oscillates in (a) and (b), but phase-winding occurs in case (c). The average temporal growth rates of both modes were found by dividing the total increment of X by the elapsed time. These are: (a) 0.567, -1.54; (b) 0.743, -1.759; (c) 1.174, -2.154. Since the period of the b-orbit is $2\pi/\varepsilon = 62.83$, initial disturbances as small as, say, $\exp(-20)$ will amplify to prominence during just part of a single period.

Just as for cases $\sigma_1 \ll 1$ examined in section 3, present cases where $\varepsilon \ll 1$ must resemble the 'bouncing' solutions of section 2 which correspond to $\varepsilon = 0$. For example, we may envisage initial states $(a, b) = (0, K)$, with K real. If $0 < K < 1 - \sigma$ or $K > 1 + \sigma$, small a-disturbances will grow, and trajectories will follow near-semicircular paths in times small compared with $2\pi/\varepsilon$. The sequence of bouncing solutions obtained for $\varepsilon = 0$ will be little changed when $\varepsilon \ll 1$ provided small a-disturbances are continuously present. Accordingly, after a known number N of 'bounces', the trajectory will reach a point with $a = 0$, and with b within the stable circle with centre 1 and radius σ. Thereafter, b will slowly change its phase, as $\exp(i\varepsilon t)$, until it crosses the circular boundary; thereafter, a-disturbances will grow. Is unclear whether there will be further 'bounces', before the trajectory reaches its final resting place at one of the two fixed points $(\pm a_0, b_0)$ given by (7).

To clarify the nature of the final approach, the stability of the points (7) was examined. Gu & Sethna (1987), in treating more general cases with detuning of the forcing, already found them to be stable; a result that we here confirm. Small perturbations about $(\pm a_0, b_0)$, with exponential time dependence as $\exp(\lambda t)$, are found after reduction to have

$$[\lambda^2 + \sigma\lambda + 2\varepsilon(1 - \sigma^2)^{1/2}]^2 = \lambda^2(\sigma^2 - \varepsilon^2) - 2\varepsilon^2\sigma\lambda.$$

Though the four roots can be stated explicitly, it is enough to give their leading-order terms when ε is small. These are

$$\lambda_1 = -2\sigma + O(\varepsilon), \qquad \lambda_2 = -\varepsilon\sigma^{-1}(1 - \sigma^2)^{1/2} + O(\varepsilon^2),$$
$$\lambda_{3,4} = \pm(2\varepsilon)^{1/2}i[(1 - \sigma^2)^{1/4} + \varepsilon/4] - \varepsilon^2(4\sigma)^{-1} + O(\varepsilon^{5/2}). \qquad (9)$$

Both λ_1 and λ_2 are real and negative, while λ_3 and λ_4 are a complex-conjugate pair with negative real part. The latter roots have rather small $O(\varepsilon^2)$ decay rate.

When b exactly equals b_0, it is found that

$$(d/dt)[a_r(1 - \sigma)^{1/2} + a_i(1 + \sigma)^{1/2}] = -2\sigma[a_r(1 - \sigma)^{1/2} + a_i(1 + \sigma)^{1/2}],$$

which shows that either a approaches zero as $\exp(-2\sigma t)$, or the phase of a rapidly approaches θ_0 $= \tan^{-1}\{-(1 - \sigma)^{1/2}(1 + \sigma)^{-1/2}\}$. The a-disturbances with phase θ_0 are least-rapidly damped.

Now suppose that $a = \varepsilon^{1/2}R\exp(i\theta)$, $b = S\exp(i\phi)$, where R, S θ, ϕ are slowly-varying. Let $\phi = \sin^{-1}\sigma + \phi_1$, $\theta = \theta_0 + \theta_1$, $S = S_0 + S_1$, where ϕ_1, θ_1 and S_1 are assumed small, and $S_0 = (1 - \sigma^2)^{1/2}$, the modulus of b_0. Since $2\theta_0 + \sin^{-1}\sigma = -\pi/2$, one finds from the full equations (6) that

$$dR/dt = R(1 - \sigma^2)^{1/2}(2\theta_1 + \phi_1) + \text{h.o.t.}, \qquad d\theta_1/dt = -2\sigma\theta_1 + \text{h.o.t.},$$

$$dS_1/dt = -\varepsilon R^2(2\theta_1 + \phi_1) + \text{h.o.t.}, \qquad d\phi_1/dt = \varepsilon[1 - R^2((1 - \sigma^2)^{1/2}] + \text{h.o.t.}$$

To suppress the rapidly-decaying mode, one must choose $\theta_1 = 0$. The scaling $R = (1 - \sigma^2)^{1/4}\eta$, $\phi_1 = \varepsilon^{1/2}(1 - \sigma^2)^{-1/4}\xi$, $t = \varepsilon^{-1/2}(1 - \sigma^2)^{1/4}\tau$ then gives

$$d\xi/d\tau = 1 - \eta^2, \qquad d\eta/dt = \xi\eta. \qquad (10)$$

for which S_1 is unimportant at this order. This simple system has well-known closed orbits. At this order of approximation, the phase of a and the amplitude of b are fixed, while the modulus of a and the phase of b display nonlinear oscillations about the stable fixed point. Though the oscillations must, in fact, be weakly damped in accord with the linear result (9), it is only at higher order in ε that the slow decay is manifest.

When the initial magnitude of a is sufficiently *small*, trajectories starting close to the origin of (ξ, η) may eventually grow to violate the assumed scaling: it is then possible that the (a, b) trajectory will exhibit further 'bounces' before the final stationary point is reached. But when the above scaling is justified, a final spiralling approach to the stationary point is to be expected.

References

G.K. Forster & A.D.D. Craik, Second-harmonic resonance with Faraday excitation. *Wave Motion* **26**, 361-377 (1997).

X.M. Gu & P.R. Sethna, Resonant surface waves and chaotic phenomena. *J. Fluid Mech.* **183**, 543-565 (1987).

J.W. Miles, Nonlinear Faraday resonance. *J. Fluid Mech.* **146**, 285-302 (1984).

J.W. Miles, Parametric excitation of an internally resonant double pendulum. *J. Appl. Math. & Phys. (Z.A.M.P.)* **36**, 337-345 (1985).

D.M. Henderson & J.W. Miles, Faraday waves in 2:1 internal resonance. *J. Fluid Mech.* **222**, 449-470 (1991).
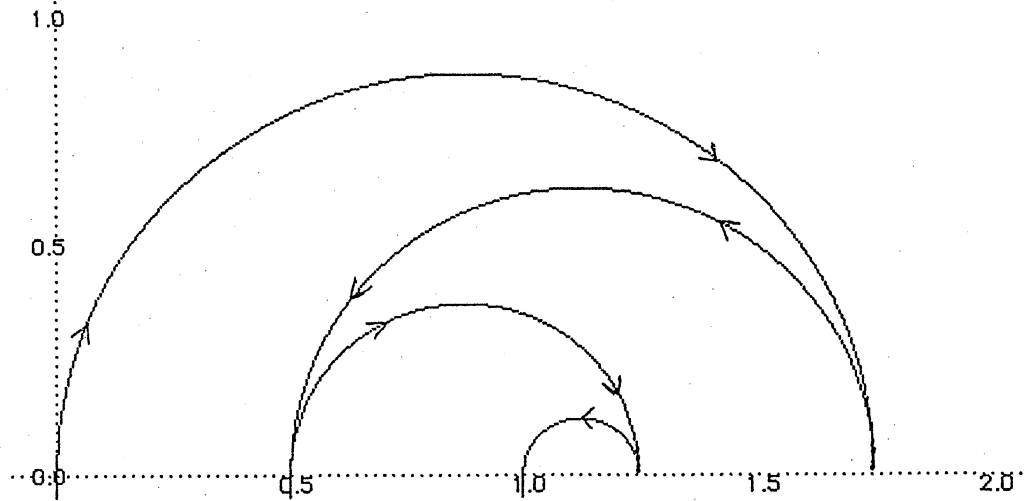
Figure 1. Semi-circular four-"bounce" trajectory, for $\sigma = 1/8$, $\sigma_1 = 0$, with initial values close to $(0, 0)$. The horizontal axis is (real) b. Clockwise "bounces" are for (b, a) (with a real); anticlockwise "bounces" are for (b, a') (with $a = ia'$ imaginary).
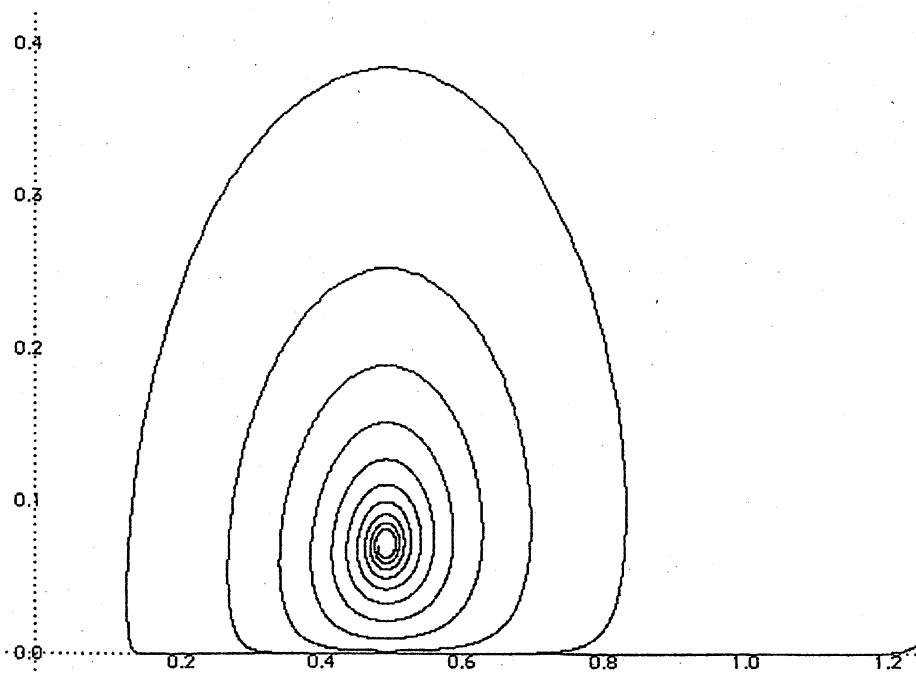

Figure 2. The approach to the stationary point, for $\sigma = 0.5$, $\sigma_1 = 0.01$. The trajectory starts near $b = 1.2$, with a very small real value of a.
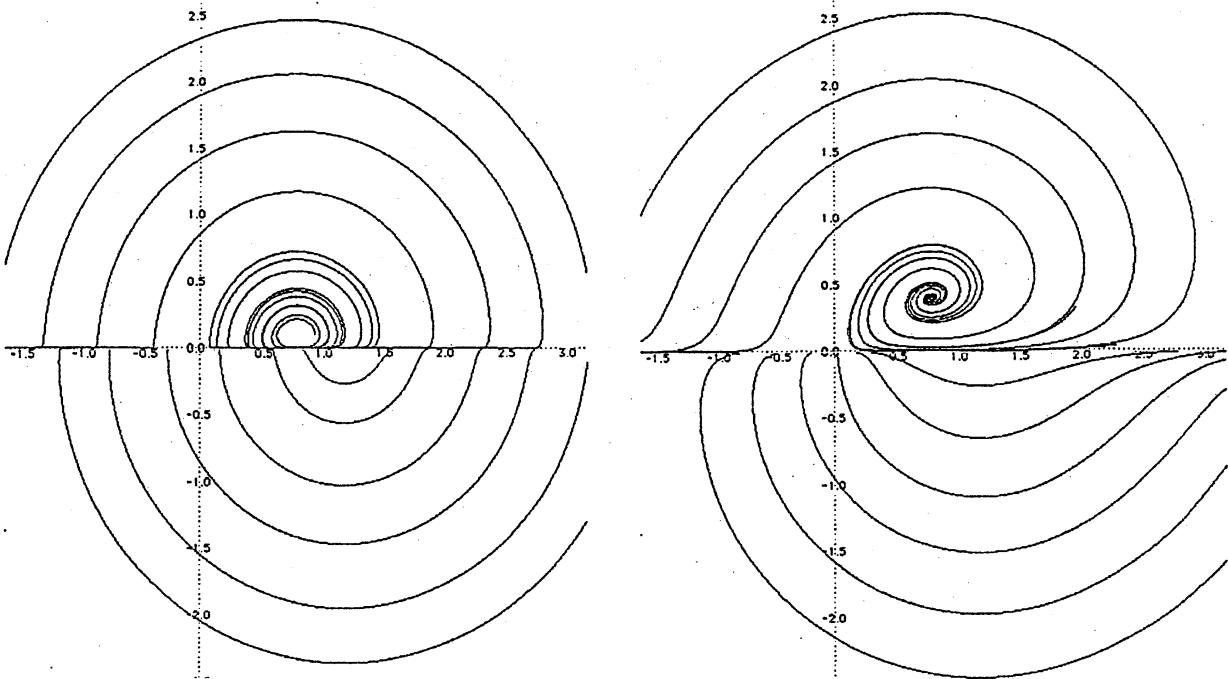
Figure 3. (a) Some computed trajectories for $\sigma = 0.2$ and $\sigma_1 = 0.01$. The near-semicircular structure resembles cases with $\sigma_1 = 0$, except close to the spiral sink. The horizontal axis denotes real b; the positive vertical axis denotes wholly-real a; and the negative vertical axis denotes the magnitude of purely imaginary a. (b) Corresponding trajectories for the more highly-damped case $\sigma = \sigma_1 = 0.2$, with spiral sink at $(0.4, 0.8)$.
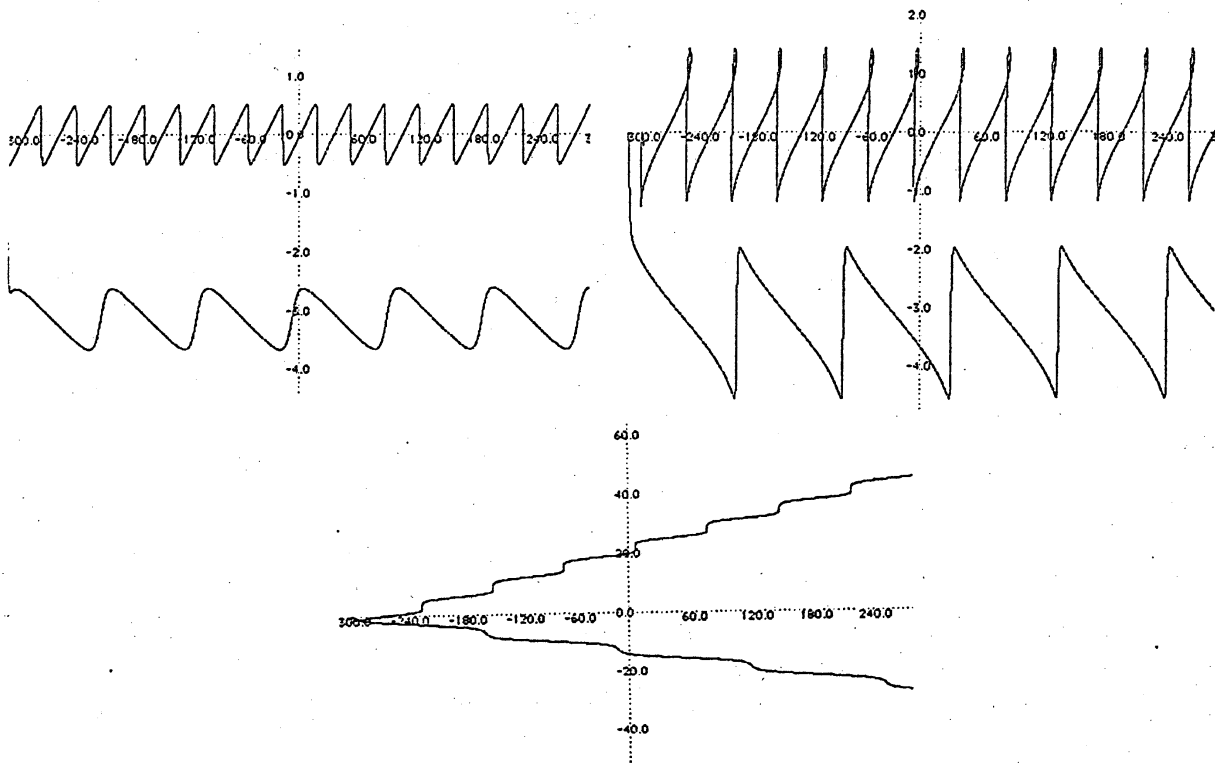
Figures 4a,b,c. Trajectories (X, Y) from (8), for $K = 0.5$, 1.0 and 1.5 respectively, with $\sigma = 0.5$ and $\varepsilon = 0.1$. Upper curves are growing modes, and lower curves decaying modes.